European Respiratory Society Congress. September 15–19, 2018, Paris, France.
5. Masekela R, Smith S, Stanojevic S, MacGinty R, Mphahlele R, Gray D. The validation of the GLI2012 'other' reference equation in Black and mixed-race South Africans: the Paediatric and Adult African Spirometry (PAAS)II study. Presented at the American Thoracic Society International Conference Abstracts. May 15–20, 2020, Philadelphia, PA.
6. Statistics South Africa. Statistical release P0302: mid-year population estimates, South Africa 2005 [Internet]. Pretoria, South Africa: Statistics South Africa; 2005 [accessed 2020 May 28]. Available from: http://www.hst.org.za/indicators/StatsSA/midyearpop2005.pdf.
7. Quanjer PH, Stocks J, Cole TJ, Hall GL, Stanojevic S; Global Lungs Initiative. Influence of secular trends and sample size on reference equations for lung function tests. *Eur Respir J* 2011;37: 658–664.
8. Miller A. Lung function testing: selection of reference values and interpretative strategies. *Am Rev Respir Dis* 1992;146:1368–1369.
9. Arigliani M, Canciani MC, Mottini G, Altomare M, Magnolato A, Loa Clemente SV, *et al*. Evaluation of the global lung initiative 2012 reference values for spirometry in African children. *Am J Respir Crit Care Med* 2017;195:229–236.
10. Ratomaharo J, Linares Perdomo O, Collingridge DS, Andriamihaja R, Hegewald M, Jensen RL, *et al*. Spirometric reference values for Malagasy adults aged 18-73 years. *Eur Respir J* 2015;45:1046–1054.
11. Madanhire T, Ferrand RA, Attia EF, Sibanda EN, Rusakaniko S, Rehman AM. Validation of the global lung initiative 2012 multi-ethnic spirometric reference equations in healthy urban Zimbabwean 7-13 year-old school children: a cross-sectional observational study. *BMC Pulm Med* 2020;20:56.
12. Fawibe AE, Odeigah LO, Saka MJ. Reference equations for spirometric indices from a sample of the general adult population in Nigeria. *BMC Pulm Med* 2017;17:48.
13. Masekela R, Hall GL, Stanojevic S, Sartorius B, MacGinty R, Saad HB, *et al*. An urgent need for African spirometry reference equations: the Paediatric and Adult African Spirometry study. *Int J Tuberc Lung Dis* 2019;23:952–958.

Supraglottic Lung Microbiome Taxa Are Associated with Pulmonary Abnormalities in an HIV Longitudinal Cohort

To the Editor:

Lung microbiome analysis of acellular BAL suggests the presence of two distinct lung pneumotypes, background predominant taxa (BPT) and supraglottic predominant taxa (SPT) (1, 2). The latter has been shown to be associated with a distinct metabolic profile and a T-helper cell type 17 proinflammatory phenotype among healthy individuals (2). We have previously demonstrated an altered lung microbiome in HIV-infected subjects, including persistent increases in taxa associated with pneumotype$_{SPT}$ (3). However, the lung inflammatory profile and associated lung function has not been elucidated. In this work, we investigated associations between lung function, inflammation, and lung microbiome dysbiosis in an HIV-positive population with relatively advanced disease who were studied at baseline and over a 1-year follow-up.

Our study population consisted of 30 HIV-infected, treatment-naive adults who underwent analysis of lung inflammatory mediators and pulmonary function testing before antiretroviral therapy (ART) and again at 4 weeks and 1 year after starting ART (3). As previously reported (3), these subjects had advanced HIV disease at baseline (median and interquartile range of CD4 is 280 and 92–385) and had sustained viral control and improved CD4 counts after starting ART. Forty-eight genera had a relative abundance $\geq$2% and were included in this analysis. Taxa were then classified as either BPT or SPT based on previous classification (1, 2). Taxa not classified in these prior reports were included in the SPT group if they were known common oropharyngeal organisms. Taxa not described in these reports were placed in the BPT group if prior published work demonstrated they were not common oral taxa or left as unclassified or not defined taxa if no data were available linking them to a human compartment. In general, pneumotype$_{SPT}$ was dominated by supraglottic phyla such as *Bacteroidetes*, *Firmicutes*, and *Fusobacterium*, whereas pneumotype$_{BPT}$ was enriched with background predominant phyla such as *Proteobacteria* and *Actinobacteria*. The pairwise correlation between genera at baseline (before ART) and at 4 weeks and 1 year after ART is shown in Figure 1. Most (>80%) pairwise correlations between taxa within the pneumotype$_{SPT}$ subgroup were positive (Figures 1A–1C). Correlations between pneumotype$_{BPT}$ taxa were weaker, and the majority of the correlations between pneumotype$_{SPT}$ and pneumotype$_{BPT}$ were negative for all three time points. The negative correlation between pneumotype$_{SPT}$ and pneumotype$_{BPT}$ increased after receiving ART. These data suggest that taxa within pneumotype$_{SPT}$ are relatively uniform and stable over time, reflecting organisms found in the oral cavity. In contrast, taxa within pneumotype$_{BPT}$ are much more variable and likely influenced by environmental factors. Consistent with prior reports (4), adjusting for smoking had no significant effects on the respiratory microbiome.

A weighted Spearman correlation for repeated measures, using the number of observations as weights, was used to assess the association of taxa abundance with inflammatory markers as well as with lung function measurements (5). With the exception for *Granulicatella*, pneumotype$_{SPT}$ taxa were positively associated with BAL proinflammatory cytokines (Table 1, top panel). It is worth noting that *Tropheryma*, which would be classified as BPT as it is not a typical supraglottic organism (6), was associated with greater inflammation. The only other pneumotype$_{BPT}$ organism associated with lung inflammation was *Moraxella*, a known respiratory tract pathogen. Eleven genera were significantly associated with at least one spirometry or diffusion capacity measurement (i.e., FEV_1; FVC; forced expiratory flow, midexpiratory phase; and D_{LCO} corrected for hemoglobin

H.L.T. is supported by NIH grant U01HL098960; K.S.K. by NIH grant R01HL83468; and J.J.Z. by NIH grants K01DK106116, 1R21HL150374-01A1, and 2R01HG006139-08A1 and an Arizona Biomedical Research Commission grant. H.Z. is partially supported by NIH grants HG006139 and GM53275 and National Science Foundation grant DMS-1645093, and Y.C. is partly supported by NIH grants ES027013, ES028889, and AI39439.

Author Contributions: Conception and design: J.J.Z., J.Z., K.S.K., and H.L.T. Analysis and interpretation: J.J.Z., J.Z., H.Z., Y.C., S.G., G.M.W., K.S.K., and H.L.T. Drafting the manuscript for important intellectual content: J.J.Z., J.Z., H.Z., Y.C., S.G., G.M.W., K.S.K., and H.L.T. Data generation and quality control: I.R., G.M.W., E.W., Q.D., K.S.K., H.L.T.

Originally Published in Press as DOI: 10.1164/rccm.202004-1086LE on August 12, 2020

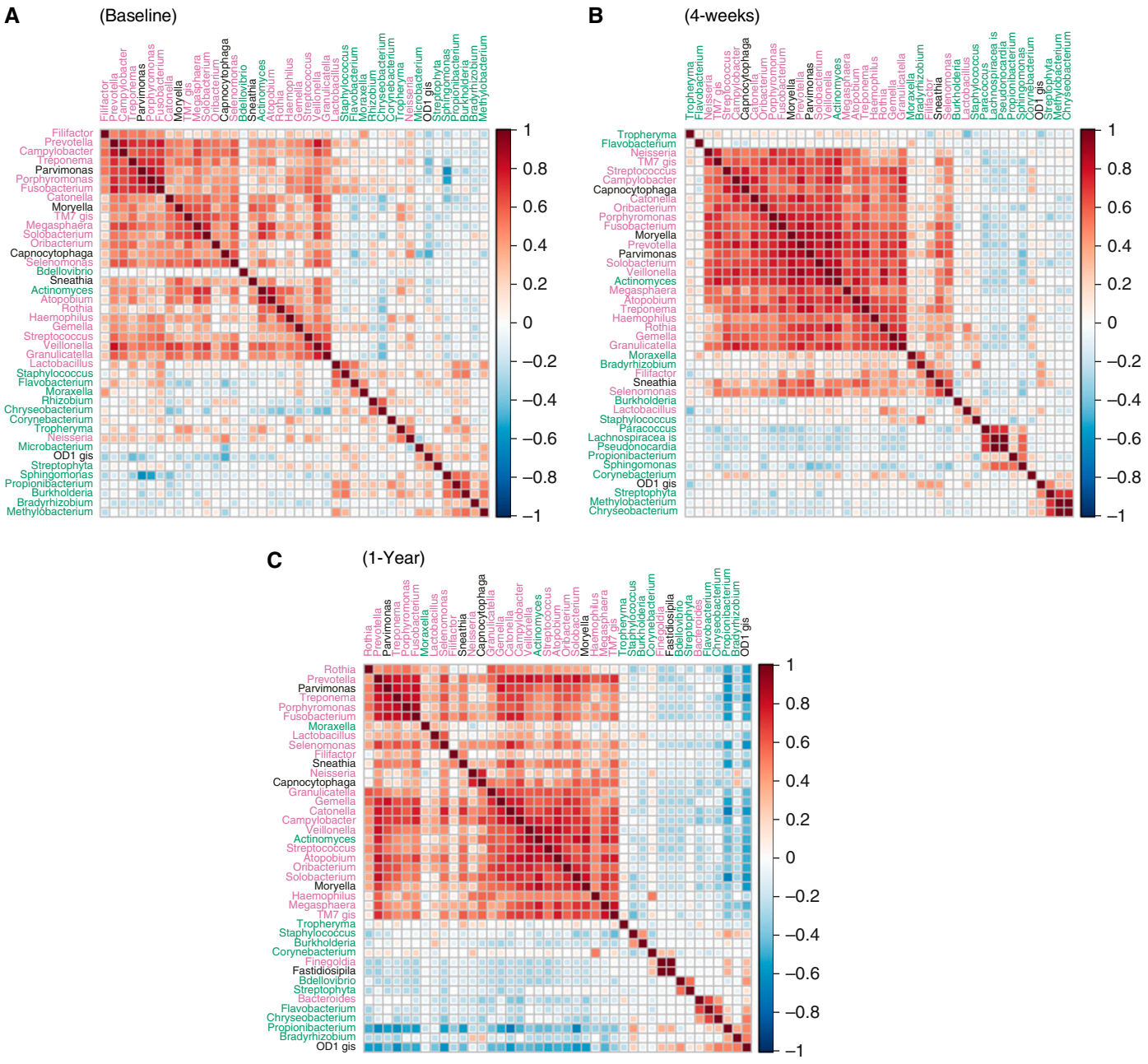

Figure 1. Heat map of Spearman correlation between genera at (*A*) baseline. (*B*) Four weeks after baseline. (*C*) One year after baseline. Spearman's ρ correlation matrix was reordered by the hierarchical clustering algorithm with complete agglomeration. Red color represents positive correlation, whereas blue color shows negative correlation. Genera in pneumotype$_{BPT}$ are in dark cyan font, and genera in pneumotype$_{SPT}$ are in dark pink font. Dark gray font represents not defined pneumotype taxa. (*D*) A cooccurrence network of genus-level taxa generated by the SparCC (Sparse Correlation for Compositional Data) package and visualized by Cytoscape 3.2.6. Cooccurrences were assessed by significant weighted Spearman's ρ calculated using all time points with permutation $P < 0.05$ and $\rho > 0.6$. Genera identified as pneumotype$_{BPT}$ are in light blue, and genera identified as pneumotype$_{SPT}$ are in light pink. The undefined genera are in light gray. The lung function parameters and inflammation markers are in yellow and purple, respectively. The dark red line indicates the positive association; the green line indicates the negative association. BPT = background predominant taxa; DsbHb = D_{LCO} corrected for hemoglobin; FEF = forced expiratory flow; IP-10 = IFN-inducible protein 10; MCP-1 = monocyte chemoattractant protein-1; SPT = supraglottic predominant taxa.

shown in Table 1, bottom panel). Among them, six genera were pneumotype$_{SPT}$, three were pneumotype$_{BPT}$, and two did not belong to either group. Overall, pneumotype$_{BPT}$ genera *Burkholderia* and *Propionibacterium* were significantly associated with better lung function in both spirometry and diffusion capacity. In contrast, except *Neisseria*, pneumotype$_{SPT}$ taxa were associated with poorer lung function. Finally, we constructed a cooccurrence network using the SparCC (Sparse Correlation for Compositional Data) package (7)

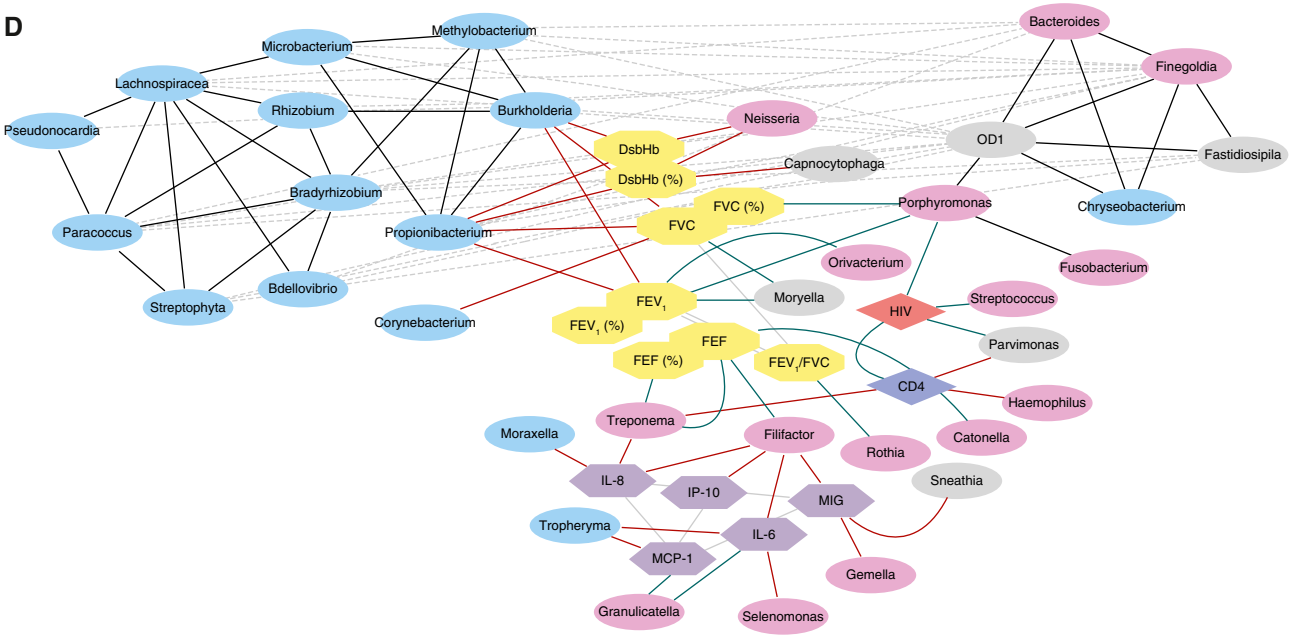

Figure 1. (*Continued*).

among genus-level taxa with significant associations with inflammatory cytokines, chemokines, and pulmonary function outcomes (Figure 1D). Genera within pneumotype$_{SPT}$ and pneumotype$_{BPT}$ cooccurred with each other, forming two well-defined clusters. Additionally, most genera in pneumotype$_{SPT}$ (5 out of 8) were significantly correlated with chemokine/cytokine levels. In contrast, most SPT-characteristic genera (5 out of 6) were negatively correlated with lung function except for *Neisseria*. Similar results were observed if each time point was analyzed separately.

In this study, we defined lung microbiome pneumotypes based on prior publications (1, 2). Pneumotype$_{SPT}$ taxa are likely derived from the oral cavity and supraglottic region, considered widely as representing a true lower respiratory tract microbiome that have the potential to cause local inflammation. All other taxa have traditionally been grouped in the BPT pneumotype and are felt to represent "background" organisms. Our results highlight strengths and caveats to this paradigm, particularly in the context of HIV. The significant positive correlations between oropharyngeal taxa in Figures 1A–1C strongly support the concept of a supraglottic pneumotype. The lack of correlation between BPT taxa emphasizes that in the absence of SPT taxa, the pneumotype$_{BPT}$ tends to be unique in different individuals. However, the concept that the pneumotype$_{BPT}$ represents just background taxa needs to be reexamined. First, *Tropheryma whipplei*, a pneumotype$_{BPT}$ taxa, was associated with lung inflammation. Widespread colonization of *Tropheryma* has been reported in the lungs of HIV-infected subjects and is dramatically reduced with ART (6). Although we classified *Tropheryma* as pneumotype$_{BPT}$ as it has not been found in the oral cavity when sampled from oral washings (6), this organism is known to be present in the gastrointestinal tract, where it may cause Whipple's disease. As such, *Tropheryma* is likely entering the lung compartment through the blood after translocation from the gut. *Moraxella* is another example of a taxa that was included in the BPT group but is clearly associated with lung inflammation in our cohort. *Moraxella* is a known lower respiratory tract pathogen that can cause lower airway inflammation. Even though they do not fall into the SPT category, certain groups of *Moraxella* (e.g., *Moraxella catarrhalis*) are known lung pathogens (8). These results highlight the fact that although most background taxa do not cause lung inflammation, there are instances through which bacteria not usually found in the supraglottic space may gain access to the lower respiratory tract and be associated with inflammation. The beneficial effect of some BPT taxa with lung function is intriguing. Whether this represents a true protective effect or just the absence of SPT bacteria requires further study. Finally, this work supports the paradigm that the presence of supraglottic taxa in the lower respiratory tract resulting from chronic low-grade aspiration seen in virtually all humans may be a susceptibility marker to chronic lung diseases seen in both HIV-infected subjects and non–HIV-infected aging population. This paradigm is further supported by recent work (9).

In conclusion, we demonstrated that there are significant correlations among lung microbiome composition, lower respiratory tract inflammation, and lung function in patients living with HIV. Our findings contribute to a growing body of work demonstrating correlations between the host microbiome and chronic disease (10), with implications for both the HIV-infected and HIV-uninfected population. ■

Author disclosures are available with the text of this letter at www.atsjournals.org.

Jin J. Zhou, Ph.D.*‡
Jing Zhai, Ph.D.‡
University of Arizona
Tucson, Arizona

Table 1. Genera Significantly Associated with Chemokine or Cytokine Levels and Lung Function

Pneumotype	Genus	Phylum	Chemokine or Cytokine*	Weighted Spearman's ρ (95% CI)*
BPT	*Moraxella*	*Proteobacteria*	IL-8	0.485 (0.151 to 0.719)
	Tropheryma	*Actinobacteria*	MCP-1	0.438 (0.093 to 0.690)
			IL-6	0.415 (0.064 to 0.674)
SPT†‡	*Filifactor*	*Firmicutes*	IL-8	0.662 (0.396 to 0.825)
			IP-10	0.463 (0.123 to 0.705)
			MIG	0.673 (0.413 to 0.832)
			IL-6	0.384 (0.027 to 0.654)
	Granulicatella	*Firmicutes*	MCP-1	−0.369 (−0.644 to −0.011)
			IL-6	−0.448 (−0.696 to −0.105)
	Gemella	*Firmicutes*	MIG	0.363 (0.003 to 0.639)
	Selenomonas	*Firmicutes*	IL-6	0.415 (0.064 to 0.674)
	Treponema	*Spirochaetes*	IL-8	0.434 (0.088 to 0.687)
NDT	*Sneathia*	*Fusobacteria*	MIG	0.367 (0.008 to 0.643)

Pneumotype	Genus	Phylum	Lung Function	Weighted Spearman's ρ (95% CI)*
BPT	*Burkholderia*	*Proteobacteria*	FEV_1	0.494 (0.163 to 0.725)
			FVC	0.538 (0.221 to 0.752)
			DsbHb	0.529 (0.209 to 0.747)
	Corynebacterium	*Actinobacteria*	FVC	0.433 (0.086 to 0.686)
	Propionibacterium	*Actinobacteria*	FEV_1	0.361 (0.001 to 0.638)
			FVC	0.445 (0.101 to 0.694)
			DsbHb	0.650 (0.379 to 0.819)
			DsbHb% predicted	0.569 (0.262 to 0.771)
SPT†§	*Filifactor*	*Firmicutes*	$FEF_{25–75}$	−0.419 (−0.677 to −0.069)
	Neisseria	*Proteobacteria*	DsbHb	0.490 (0.158 to 0.723)
			DsbHb% predicted	0.596 (0.301 to 0.787)
	Oribacterium	*Firmicutes*	FEV_1	−0.418 (−0.676 to −0.068)
	Porphyromonas	*Bacteroidetes*	FEV_1% predicted	−0.392 (−0.659 to −0.037)
			FVC% predicted	−0.370 (−0.644 to −0.011)
	Rothia	*Actinobacteria*	FEV_1/FVC	−0.422 (−0.679 to −0.072)
	Treponema	*Spirochaetes*	$FEF_{25–75}$	−0.440 (−0.691 to −0.094)
			FEF% predicted	−0.475 (−0.713 to −0.139)
NDT	*Moryella*	*Firmicutes*	FEV_1	−0.368 (−0.643 to −0.008)
			FVC	−0.410 (−0.671 to −0.058)
	Capnocytophaga	*Bacteroidetes*	DsbHb% predicted	0.411 (0.059 to 0.672)

Definition of abbreviations: BPT = background predominant taxa; CI = confidence interval; DsbHb = D_{LCO} corrected for hemoglobin; FEF = forced expiratory flow; $FEF_{25–75}$ = forced expiratory flow, midexpiratory phase; IP-10 = IFN-inducible protein 10; MCP-1 = monocyte chemoattractant protein-1; NDT = not defined taxa; SPT = supraglottic predominant taxa.

*Weighted Spearman's ρ that are larger than 2 SDs from mean were shown in the table.

†A permutation test was adopted to evaluate the enrichment of positive or negative associations (defined by Spearman's ρ with larger than 2 SDs from mean) among SPT genera with chemokine/cytokine or lung function levels. Ten thousand permutation replicates were used.

‡Permutation $P = 0.082$.

§Permutation $P < 0.000$.

Hua Zhou, Ph.D.
University of California, Los Angeles
Los Angeles, California

Yin Chen, Ph.D.
Stefano Guerra, M.D.
Ian Robey, Ph.D.
University of Arizona
Tucson, Arizona

George M. Weinstock, Ph.D.
Erica Weinstock, Ph.D.
Jackson Laboratory for Genomic Medicine
Farmington, Connecticut

Qunfeng Dong, Ph.D.
Loyola University Chicago
Maywood, Illinois

Kenneth S. Knox, M.D.
University of Arizona College of Medicine-Phoenix
Phoenix, Arizona

Homer L. Twigg III, M.D.
Indiana University Medical Center
Indianapolis, Indiana

ORCID ID: 0000-0001-7983-0274 (J.J.Z.).

*Corresponding author (e-mail: jzhou@email.arizona.edu).
‡These authors contributed equally to this work.

References

1. Segal LN, Alekseyenko AV, Clemente JC, Kulkarni R, Wu B, Gao Z, *et al*. Enrichment of lung microbiome with supraglottic taxa is associated with increased pulmonary inflammation. *Microbiome* 2013;1:19.

2. Segal LN, Clemente JC, Tsay JC, Koralov SB, Keller BC, Wu BG, *et al*. Enrichment of the lung microbiome with oral taxa is associated with lung inflammation of a Th17 phenotype. *Nat Microbiol* 2016;1:16031.
3. Twigg HL III, Knox KS, Zhou J, Crothers KA, Nelson DE, Toh E, *et al*. Effect of advanced HIV infection on the respiratory microbiome. *Am J Respir Crit Care Med* 2016;194:226–235.
4. Morris A, Beck JM, Schloss PD, Campbell TB, Crothers K, Curtis JL, *et al*.; Lung HIV Microbiome Project. Comparison of the respiratory microbiome in healthy nonsmokers and smokers. *Am J Respir Crit Care Med* 2013;187:1067–1075.
5. Bland JM, Altman DG. Calculating correlation coefficients with repeated observations: part 2. Correlation between subjects. *BMJ* 1995;310: 633.
6. Lozupone C, Cota-Gomez A, Palmer BE, Linderman DJ, Charlson ES, Sodergren E, *et al*.; Lung HIV Microbiome Project. Widespread colonization of the lung by Tropheryma whipplei in HIV infection. *Am J Respir Crit Care Med* 2013;187:1110–1117.
7. Friedman J, Alm EJ. Inferring correlation networks from genomic survey data. *PLOS Comput Biol* 2012;8:e1002687.
8. Narinesingh SP, Whitby DJ, Davenport PJ. Moraxella catarrhalis: an unrecognized pathogen of the oral cavity? *Cleft Palate Craniofac J* 2011;48:462–464.
9. Yang L, Dunlap DG, Qin S, Fitch A, Li K, Koch CD, *et al*. Alterations in oral microbiota in HIV are related to decreased pulmonary function. *Am J Respir Crit Care Med* 2020;201:445–457.
10. Gilbert JA, Quinn RA, Debelius J, Xu ZZ, Morton J, Garg N, *et al*. Microbiome-wide association studies link dynamic microbial consortia to disease. *Nature* 2016;535:94–103.

Anti-FXa Activity with Intermediate-Dose Thromboprophylaxis in COVID-19

To the Editor:

We read with interest the article by Dutt and colleagues describing measurement of anti–factor Xa (FXa) activity in ward patients with coronavirus disease (COVID-19) as well as those requiring intensive care (1). The authors suggest that patients admitted to an ICU with COVID-19 may warrant a higher starting dose of pharmacological thromboprophylaxis, although the optimal dose in these patients is uncertain pending upcoming randomized controlled trials. Current guidelines from various medical societies suggest routine pharmacological thromboprophylaxis in patients with COVID-19. However, there is a lack of consensus on whether standard-dose or higher intermediate-dose thromboprophylaxis should be used (2–5). We would like to present our experience with measuring anti-FXa activity using a higher, weight-based dose of enoxaparin for thromboprophylaxis. This retrospective observational study was deemed exempt by our institutional review board.

In early April, we noticed a high rate of thrombosis and thromboembolism among critically ill patients with COVID-19, an observation consistent with those in other institutions (6–8). Therefore, we adopted intermediate-dose thromboprophylaxis for critically ill patients with COVID-19 with enoxaparin (0.5 mg/kg twice daily), as described in Table 1, as our new standard of care. The dosages were selected based on several single-center studies suggesting higher rates of attainment of target anti-FXa activity with higher-dose enoxaparin (9, 10). Importantly, the target anti-FXa activity for pharmacologic prophylaxis is not evidence based, and adjusting doses to provide higher attainment of target activity was not demonstrated to improve clinical outcomes.

We monitored anti-FXa activity for the first 40 patients receiving this dosing strategy. Anti-FXa was checked 3–4 hours after the third or fourth dose of the intermediate-dose enoxaparin regimen. The enoxaparin dose was then adjusted as necessary to achieve a target anti-FXa activity of 0.2–0.5 U/ml.

Results are shown in Table 2. Seventy-five percent ($n = 33$) of patients achieved the targeted anti-FXa activity without further dose adjustment. Twenty-five percent ($n = 11$) of patients had their dose adjusted from institutional guideline recommended doses at some point in their hospitalization. Only three patients had dose adjustment because of their anti-FXa activity, with decreased dosage for two patients, one of whom later developed venous thromboembolism. Only two patients had enoxaparin decreased or stopped because of bleeding (hematuria in both cases). Four patients had their dosages increased to a therapeutic regimen because of clinically suspected ($n = 2$) or confirmed ($n = 2$) clotting events. Both patients with confirmed clotting events and one patient with a suspected clotting event were initially on standard-dose thromboprophylaxis before the institutional transition to intermediate-dose thromboprophylaxis.

We achieved a high rate of the targeted anti-FXa activity using this intermediate dosing scheme. Most patients outside the target anti-FXa range were above rather than below goal concentrations. After reviewing this data, our institution decided to continue intermediate-dose thromboprophylaxis but eliminate routine anti-FXa monitoring because it rarely resulted in dose adjustments. Only 2 of the 10 patients with anti-FXa activity of greater than 0.5 U/ml were decreased because of this monitoring, which was likely due to concern over the high rates of thromboembolic complications in this population. In addition, anti-FXa monitoring for thromboprophylaxis is controversial, especially in intensive care (11–13). There is no clear relationship between anti-FXa activity and the safety or efficacy of thromboprophylaxis. Although low anti-FXa activity has been associated with thromboembolism, there is no proven benefit to adjusting the enoxaparin dose to a "target" anti-FXa activity. Furthermore, the target anti-FXa activity of 0.2–0.5 U/ml has not been rigorously validated.

In conclusion, our results may assist others considering intermediate-dose thromboprophylaxis and anti-FXa monitoring in critically ill patients with COVID-19. Our findings suggest that intermediate-dose thromboprophylaxis led to anti-FXa activity according to predefined criteria in most of

Author Contributions: Conception and design: S.H.R., J.M.C., S.D., K.M.M., P.P., D.C.K., A.P.P., C.M.Q., and C.M.G. Data collection: S.H.R., J.M.C., S.D., and K.M.M. Analysis and interpretation: S.H.R., J.M.C., S.D., K.M.M., P.P., D.C.K., and C.M.G. Drafting and revision of the manuscript: S.H.R., J.M.C., S.D., K.M.M., P.P., D.C.K., A.P.P., C.M.Q., and C.M.G.

Originally Published in Press as DOI: 10.1164/rccm.202006-2511LE on September 15, 2020